

## Surface Reactions of 3-Butenenitrile on the Si(001)-2 × 1 Surface at Room Temperature

Sylvie Rangan, Fabrice Bournel, Jean-Jacques Gallet, Stefan Kubsky, Karine Le Guen, Georges Dufour, and François Rochet\*

Laboratoire de Chimie Physique Matière et Rayonnement, 11 rue Pierre et Marie Curie, 75231 Paris Cedex 05, France

Fausto Sirotti

Laboratoire pour l'Utilisation du Rayonnement Electromagnetique, Centre Universitaire Paris-Sud, Bâtiment 209D, 91405 Orsay Cedex, France

Guido Piaszenski, Ralf Funke, Martin Knepe, and Ulrich Köhler

Fakultät für Physik und Astronomie, Institut für Experimentalphysik IV/Oberflächenphysik, Ruhr-Universität Bochum, NB 4/166, D-44780 Bochum, Germany

Received: April 5, 2005; In Final Form: May 16, 2005

Using a combination of local—scanning tunneling microscopy—and spatially integrated, but chemically sensitive probes—X-ray photoelectron spectroscopy and near edge X-ray absorption fine structure spectroscopy—we have examined how 3-butenitrile reacts with the Si(001)-2 × 1 surface at room temperature. Electron spectroscopies indicate three different nitrogen chemical bonds: a Si—C≡N—Si bond, a C=C=N cumulative double bond, and a C≡N moiety datively bonded to a silicon atom. All molecular imprints detected by scanning tunneling microscopy (STM) involve two adjacent silicon dimers in the same row. The three geometries we propose—a double di-σ bonding via the C≡N and the C=C, a cumulative double bond formation associated with αC—H bond dissociation, and a di-σ vinyl bonding *plus* a C≡N datively bonded to a silicon atom—are all compatible with electron spectroscopies and data. Real-time Auger yield kinetic measurements show that the double di-σ bonding geometry is unstable when exposed to a continuous flux of 3-butenitrile molecules, as the Si—C≡N—Si unit transforms into a C≡N moiety. A model is proposed to explain this observation.

## I. Introduction

The adsorption of polyfunctional organic molecules on the dimerized silicon (001) surface (Figure 1a) has attracted much attention because an understanding of the rules leading to the selective attachment of a particular “anchoring” unit to the substrate is of prime importance in the design of molecular nanodevices.  $\pi$ -Bonded functionalities, such as acetylenic ( $\text{—C}\equiv\text{C—}$ ), vinyl ( $\text{>C=C<}$ ), and cyano ( $\text{—C}\equiv\text{N}$ ) groups, are typical anchoring units that bind to the silicon dimer ( $\text{Si}_2$ ) to form cycloaddition products.<sup>1–3</sup> The competition between vinyl and cyano groups has been examined experimentally in polyfunctional molecules such as 2-propenenitrile ( $\text{H}_2\text{C=CH—C}\equiv\text{N}$ , also known as acrylonitrile)<sup>4–6</sup> and 3-butenitrile<sup>5</sup> ( $\text{H}_2\text{C=CH—CH}_2\text{—C}\equiv\text{N}$ , also known as allylcyanide). These molecules are depicted in Figure 1. A comparative study of the absorption modes of a nonconjugated molecule (3-butenitrile) versus a conjugated one (2-propenenitrile) is indeed worthy of interest: in contrast to 3-butenitrile where bond shifts are blocked by the aliphatic spacer, 2-propenenitrile has a resonant form,  $\text{H}_2\text{C}^+\text{—CH=C=N}^-$ . Therefore, 2-propenenitrile has a propensity to bridge two silicon dangling bonds via its terminal carbon and nitrogen atoms, to form a  $\text{Si—H}_2\text{C—CH=C=N—Si}$  unit. Besides cyano and vinyl anchoring, the formation of a cumulative double bond (CDB,  $\text{N=C=C}$ ) unit at 300 K is indeed indicated by near edge X-ray absorption fine structure spec-

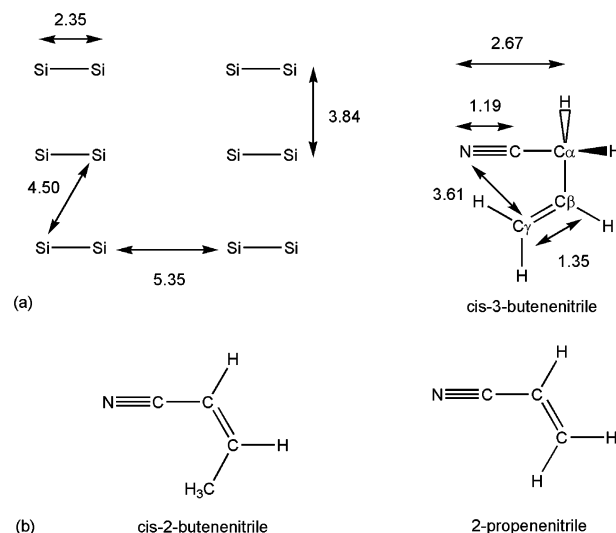


**Figure 1.** (a) Characteristic distances (in angstroms) for the reconstructed Si(100)-2 × 1 surface and for the (nonconjugated) *cis*-3-butenitrile. (b) Schemes of *cis*-2-butenitrile (conjugated isomer of *cis*-3-butenitrile) and of 2-propenenitrile (also conjugated). Note that in *cis*-3-butenitrile the αH is acidic and that the γC—N distance is 3.61 Å, close to the distance between the adjacent dimer in the same row (3.85 Å).

troscopy (NEXAFS).<sup>4,6</sup> Moreover, a characteristic CDB stretching mode at 1985  $\text{cm}^{-1}$  is reported in the infrared (IR)

\* Corresponding author. E-mail: rochet@ccr.jussieu.fr.

spectroscopy study of Schwartz and Hamers.<sup>5</sup> In comparison with 2-propenenitrile, the situation for the nonconjugated molecule 3-butenitrile should be more simple, assuming no isomerization and/or decomposition path. 3-Butenenitrile should bind to the silicon dimers by the vinyl group and/or by the cyano group, and no  $\text{N}=\text{C}=\text{C}$  formation is expected. The final bonding geometries should depend on the conformation—*cis* (*syn*), *gauche*, or *trans* (*anti*)—adopted by the molecule on the surface while adsorbed in a precursor state. For instance, the cycloaddition of both anchoring units on two adjacent silicon dimers of the same row can be envisioned on geometric considerations if the *cis* conformer is retained on the surface (in the gas phase at 20 °C, there is  $94 \pm 18\%$  *cis* conformer<sup>7</sup>). Indeed, the  $\gamma\text{C}-\text{N}$  distance is 3.61 Å, which is close to the distance between two dimers (3.85 Å). On the other hand, *gauche* and *trans* conformers should favor the bonding of only one anchoring unit.<sup>8</sup> The IR data from ref 5 point to a nearly complete attenuation of the  $\text{C}\equiv\text{N}$  stretching mode at  $2255\text{ cm}^{-1}$  after adsorption at 300 K. This was interpreted in terms of a bonding of the cyano group with the silicon surface. The absence of  $\text{C}-\text{H}$  stretching modes related to unsaturated carbons (above  $3000\text{ cm}^{-1}$ ) also pointed to an interaction of the vinyl unit with the surface. *However, the most intriguing observation was that of a medium intensity absorbance at  $1982\text{ cm}^{-1}$ , characteristic of a CDB unit.* To explain the observation of a CDB mode for this nonconjugated molecule, Schwartz and Hamers<sup>5</sup> proposed that an intramolecular hydrogen transfer (from  $\alpha\text{C}$  to  $\gamma\text{C}$ , see Figure 1) would lead to the formation of a  $\text{Si}-\text{N}=\text{C}=\text{CH}-\text{CH}(\text{CH}_3)-\text{Si}$  unit.

On the parent surface,  $\text{Ge}(001)-2 \times 1$ , exposed at room temperature to 3-butenitrile, besides other products, a CDB adduct was clearly detected by IR spectroscopy.<sup>9</sup> In contrast to the interpretation of Schwartz and Hamers,<sup>5</sup> this finding was explained by an *isomerization* of 3-butenitrile into 2-butenitrile ( $(\text{CH}_3)\text{HC}=\text{C}=\text{N}$ , see Figure 1b), over the stainless steel of the gas handling manifold before its introduction into the reaction chamber. Nevertheless, Mui and co-workers<sup>10</sup> examined theoretically—a density functional theory (DFT) calculation using a silicon cluster—the reaction paths of 3-butenitrile leading to its isomerization *on the silicon surface*. The role of the acidic  $\alpha\text{H}$  was particularly emphasized.<sup>11</sup>

We report here a study of the surface reactions of 3-butenitrile on  $\text{Si}(001)$  at 300 K, using a combination of near edge X-ray absorption fine structure spectroscopy (NEXAFS), X-ray photoemission spectroscopy (XPS), and scanning tunneling microscopy (STM). The chemical sensitivity of core-level spectroscopies (XPS/NEXAFS) allows the detection of three different adsorption modes. Adding this chemical information to the spatial information, that is, the bond orientation provided by NEXAFS and the location of the reaction sites given by atomically resolved STM, has enabled us to draw a picture of the reaction products.

## II. Experimental Section

**A. Synchrotron Radiation.** The experiments have been performed at the SB7 beamline SB7 on the experimental station ABS6 of LURE-SuperACO synchrotron facility (Orsay, France). The photon energy was calibrated using both first- and second-order light from the Dragon-type<sup>12</sup> monochromator. The degree of linear polarization of the bending magnet source was 95%. In the experimental geometry, the larger component of the electric field,  $E_{\text{hor}}$ , which lies in the horizontal orbital plane of the storage ring, is always contained in a (110) plane of the  $\text{Si}(001)$  substrate. The sample could rotate around a vertical axis

so that the angle of incidence of the photon,  $\theta$  (measured with respect to the sample surface plane), could be changed from 0° (grazing incidence) to 90° (normal incidence). Note that  $\theta$  is also equal to the angle between the electric field main component,  $E_{\text{hor}}$ , and the normal to the surface.

**XPS.** Core-level photoemission spectra were also recorded (at an electron takeoff direction normal to the surface) with a Scienta 200 hemispherical analyzer working in swept mode. The data analysis consists of a background subtraction and a standard curve fitting procedure. In the present paper, only N 1s core-level spectra are reported (the excitation energy,  $h\nu$ , was 450 eV). To help comparison to other published data, we note that the position of the Si 2p<sub>3/2</sub> core-level binding energy (BE), measured relative to the Fermi level, is at 99.5 eV after dosing.

**NEXAFS.** The Auger yield (AY) mode has been used to increase the adsorbate-to-Si bulk signal ratio.<sup>13</sup> The Scienta 200 analyzer, working in fixed mode, is used for that purpose. For N 1s NEXAFS spectra, 18 eV wide energy windows, centered at 363, 373, and 383 eV, were chosen. To obtain reasonable count rates, the photon bandwidth was around 180 meV. Angle dependent measurements have been carried out. The spectra were normalized with respect to the secondary electron photoemission peak dominated by contributions from bulk Si. Then, the “absorption jump”, measured before the edge and some 20 eV after it, was normalized to unity.

**Auger Yield Kinetic Studies.** Real-time resonant Auger yield measurements were also performed: “fast” spectra consisting of few key energies in the N 1s absorption spectrum were recorded while the surface was dosed under a constant gas pressure; typically, a pre-edge photon energy (at  $h\nu = 390\text{ eV}$ ) and a photon energy leading to a transition to the continuum (415 eV) were chosen, along with the characteristic NEXAFS  $\pi^*$  transitions of the adsorbed species. The AY measured at  $\pi^*$  transitions and at  $h\nu = 415\text{ eV}$  have been divided by the pre-edge intensity, to correct for the time variations of the photon intensity. Then, for each NEXAFS transition, the AY intensity, measured before gas introduction, is subtracted to give the corrected AY,  $\text{AY}^{\text{corr}}$ . The measurements were taken at the magic angle ( $\sim 54.7^\circ$ ), where the transition intensity is independent of the molecular orbital orientation.<sup>14</sup> Given the limited photon flux delivered by the bending magnet, *fast* N 1s photoemission was not realizable. The resonant Auger yield approach was the only practical way of measuring real-time kinetics.

**B. Scanning Tunneling Microscopy.** The STM experiments were performed at both 300 and 90 K on two different ultrahigh vacuum (UHV) setups on a surface dosed with 3-butenitrile at 300 K. All STM images were obtained in the constant current mode using a tunnel current in the range 0.3–1 nA. The sample bias with respect to the tip,  $V_b$ , was either negative (to probe the filled states) or positive (to probe the empty states).

**C. Surface Cleaning and Dosing.** The native oxide was removed from the silicon sample (phosphorus doped, resistivity  $0.003\ \Omega\text{ cm}$ ) by flashing at 1250 °C. 3-Butenenitrile was dosed through a leak-valve under constant pressure (the gauge reading being uncorrected) onto the silicon surface, cooled to room temperature. 3-Butenenitrile is a commercial product (Aldrich, purity  $\geq 98\%$ ), purified by several freeze–pump–thaw cycles. The liquid is contained in a glass vial. It has been reported that 3-butenitrile is prone to isomerize to 2-butenitrile (a conjugated molecule, see Figure 1b) when contained in a steel manifold: Filler and co-workers<sup>9</sup> saw a significant increase in the CN stretching mode infrared intensity for 2-butenitrile

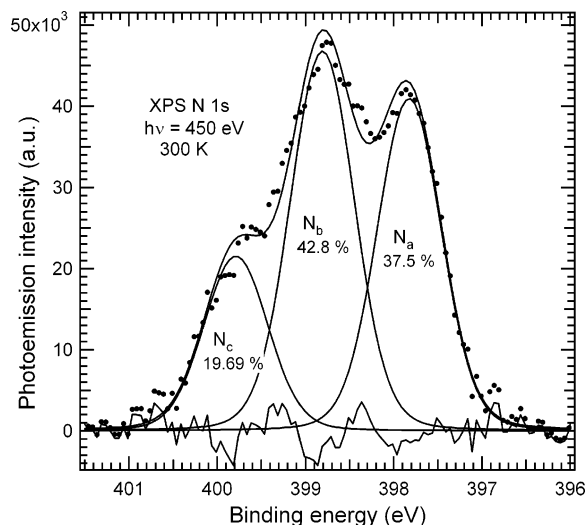


**Figure 2.** Experimental N 1s core-level spectrum (dots) of a Si(001)-2  $\times$  1 surface exposed to a dose of 6000 s  $\times$  10<sup>-8</sup> mbar at 300 K. The corresponding fits (solid curves) are also given with the weight of each contribution. The Gaussian fwhm (respectively Lorentzian fwhm) is 0.8 eV (respectively 0.1 eV).

after leaving 3-butenitrile in the steel manifold for 48 h. To avoid this transformation, the stainless steel tubes and leak-valve used to introduce 3-butenitrile in the experimental chamber were pumped before each introduction of the gas. Therefore, the residence time of 3-butenitrile in the steel manifold is equal to the duration of the exposure. Glass is inert with respect to 3-butenitrile: the gas condensed on a cooled substrate after a 9 day residence in the glass bottle exhibited the characteristic N 1s NEXAFS spectrum of a nonconjugated CN moiety (see section III.A).

### III. Results and Discussion

**A. N 1s XPS and NEXAFS Spectroscopy.** The XPS N 1s spectrum of the Si(001)-2  $\times$  1 surface, exposed at 300 K to 3-butenitrile for 6000 s under a pressure of 10<sup>-8</sup> mbar, is shown in Figure 2. With such a large dose, the maximum coverage is reached (see section III.B). The experimental spectrum is fitted by three lines— $N_a$ ,  $N_b$ , and  $N_c$ —placed at binding energies (BEs) equal to 397.8, 398.8, and 399.8 eV, respectively. Their narrow widths (0.85 eV total fwhm) suggest that each line corresponds to a single chemical state. Schwartz and Hamers<sup>5</sup> also find three spectral lines. Apart from a rigid shift of -0.1 eV, the binding energies we find are in excellent agreement with the data from ref 5. On the other hand, the  $N_a/N_b/N_c$  ratio we found (37.5:42.8:19.7) is different from that indicated in ref 5 (70:17:13).<sup>15</sup> The discrepancy may arise from the different doses and exposure times, 10<sup>-8</sup> mbar  $\times$  6000 s in the present work and 6.6  $\times$  10<sup>-8</sup> mbar  $\times$  100 s in ref 5. As it will be shown in section III.B, the distribution of the reaction products varies with the exposure time.

The N 1s NEXAFS spectra of a Si(001) surface exposed to 3-butenitrile at 300 K for various doses are given in Figures 3 and 4. In the inset of Figure 3, we present the N 1s NEXAFS spectrum of solid 3-butenitrile (a multilayer condensed on a silicon substrate cooled at 110 K, corresponding to a dose of 10<sup>-7</sup> mbar  $\times$  1800 s). A unique, narrow,  $\pi^*$  resonance is found peaked at 399.75 eV. If isomerization to 2-butenitrile (CH<sub>3</sub>-CH=CH-C $\equiv$ N) occurs, the cyano and vinyl units are conjugated, and the doubly degenerate  $\pi^*$  levels of the cyano group necessarily split into a manifold of three  $\pi^*$  levels (see, e.g., the NEXAFS spectrum of 2-propenenitrile<sup>4</sup>), which is not

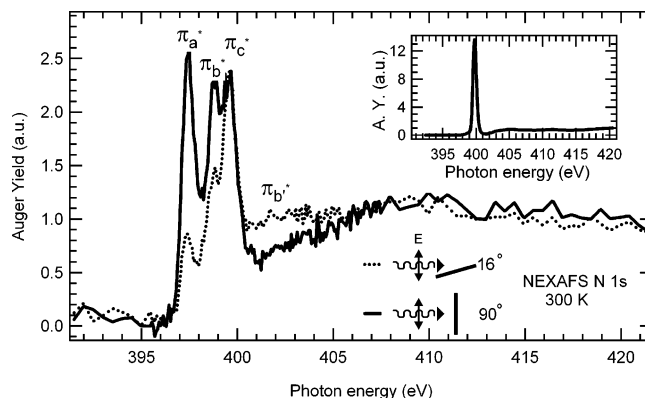


**Figure 3.** N 1s NEXAFS spectra of a surface exposed to 960 s  $\times$  2  $\times$  10<sup>-8</sup> mbar at 300 K, measured in normal incidence ( $\theta = 90^\circ$ ,  $E_{\text{hor}}$  parallel to the surface plane) and in grazing incidence ( $\theta = 16^\circ$ ,  $E_{\text{hor}}$  close to the normal to the surface). The curves are normalized to an equal "jump" before the adsorption edge (394 eV) and 20 eV after. Transitions  $\pi_a^*$  and  $\pi_b^*$  are polarized in the surface plane, and  $\pi_b^*$  is polarized perpendicularly to the surface.  $\pi_c^*$  has no clear incidence angle dependence. NEXAFS transitions energies and their assignment are given in Table 1. In the inset, we give the N 1s NEXAFS spectrum of solid 3-butenitrile, exhibiting a single  $\pi^*$  transition at 399.75 eV.

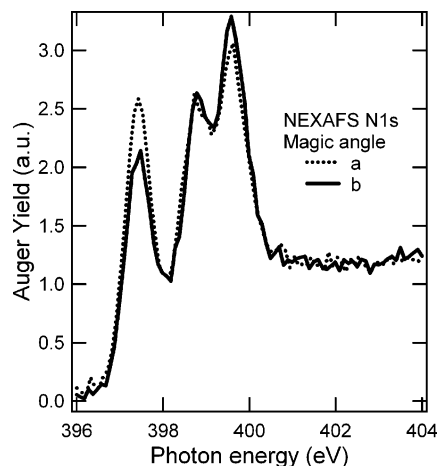


**Figure 4.** N 1s NEXAFS spectra measured at the magic angle. Curve a is measured at a base pressure of 10<sup>-10</sup> mbar, following an exposure of 1080 s  $\times$  10<sup>-8</sup> mbar; curve b is measured after an extra exposure of 8000 s  $\times$  10<sup>-8</sup> mbar (total exposure time 9080 s).

observed in the present case. The concentration of 2-butenitrile possibly contained in the multilayer film is therefore below the detection limit of NEXAFS, for the product has been contained in an inert glass vial (see section II.C) and its residence in the steel manifold has been limited to 30 min. The N 1s NEXAFS spectrum of 3-butenitrile adsorbed at room temperature (Figure 3), after an exposure of 960 s under 2  $\times$  10<sup>-8</sup> mbar, displays substantial changes with respect to that of the multilayer. Four low lying bound-state transitions (below roughly  $\sim$ 405 eV) of antibonding  $\pi^*$  character are now clearly distinguished. Three narrow  $\pi^*$  resonances (0.84 meV fwhm) are found at photon energies equal to 397.4 ( $\pi_a^*$ ), 398.6 ( $\pi_b^*$ ), and 399.6 eV ( $\pi_c^*$ ), followed by a broader structure centered at  $\sim$ 402 eV ( $\pi_b^*$ ). An absorption dichroism is clearly observed when one compares the spectrum taken at normal incidence ( $E_{\text{hor}}$  is contained in the surface plane) with that measured at grazing incidence ( $E_{\text{hor}}$  makes an angle of  $16^\circ$  with respect to the normal to the surface). This is due to the preferential spatial orientations of the adsorbate molecular bonds. (Because of the application of dipolar selection rules, the intensity of the transition is maximum when the electric field of the linearly polarized



**TABLE 1: Comparison of Calculated IP and NEXAFS Transitions for Acetonitrile Adsorbed on Si(001)-2 × 1 with the XPS Binding Energies and NEXAFS Transitions Energies Measured after 3-Butenenitrile Adsorption on the Si(001)-2 × 1 Surface [We Give Also the Calculated IPs (Acetonitrile Case, Indicated by †) and the Measured XPS Line Energies (3-Butenenitrile Case, Indicated by #) Relative to the Si-C≡N-Si Unit]**

acetonitrile (theoretical excitation energies) <sup>17</sup>			3-butenenitrile (experimental, this work)		
chemical unit	IP (eV)	NEXAFS (eV)	XPS binding energy (eV)	NEXAFS photon energy (eV)	assignment
Si-C≡N-Si	403.3 (0) <sup>†</sup>	397.98	<i>N<sub>a</sub></i> 397.8 (0) <sup>#</sup>	$\pi_a^*$ 397.5	Si-C≡N-Si
Si-N=C=C-CH <sub>2</sub>	404.5 (1.2) <sup>†</sup>	399.3	<i>N<sub>b</sub></i> 398.8 (1) <sup>#</sup>	$\pi_b^*$ 398.7	N=C=C
		402.2		$\pi_b^*$ ~402	
Si-CH <sub>2</sub> -C≡N	404.7 (1.4) <sup>†</sup>	399.7			
-C≡N datively bonded with Si	405.7 (2.4) <sup>†</sup>	399.6	<i>N<sub>c</sub></i> 399.8 (2) <sup>#</sup>	$\pi_c^*$ 399.6	-C≡N datively bonded with Si
		400.2			

radiation is parallel to the  $p$  final state and zero when it is perpendicular.<sup>16</sup>) The  $\pi_a^*$  and  $\pi_b^*$  orbitals are clearly contained in the surface plane, while  $\pi_b^*$  is perpendicular to the surface normal.  $\pi_c^*$  does not have a marked dichroic behavior.

Our attribution of NEXAFS transition energies and binding energies is based on a recent theory-assisted experimental work we carried out on the parent system acetonitrile on Si(001)-2 × 1.<sup>17</sup> DFT, within the  $\Delta$ Kohn–Sham framework, was used to calculate the N 1s ionization potential (IP) and NEXAFS transition energies of the following CH<sub>3</sub>C≡N adsorption geometries:

(i) A bonding via the C≡N group on a silicon dimer, leading to the formation of a Si-N=C-Si unit.

(ii) A bonding via the nitrogen atom with a hydrogen transferred from the molecule to the substrate, leading to the formation of a CDB unit: Si-N=C=CH<sub>2</sub>.

(iii) A bonding via a carbon atom, leading to a free C≡N: Si-CH<sub>2</sub>-C≡N.

(iv) A Si-CH<sub>2</sub>-C≡N adduct (as in case iii) whose N end is datively bonded to an adjacent silicon.

The corresponding calculated transition energies and IPs are collected in Table 1. The lower IP is calculated for the Si-C≡N-Si unit. The IP of the CDB, of the free cyano, and of the datively bonded cyano, referred to that of the Si-C≡N-Si, are shifted to higher energy by 1.2, 1.4, and 2.4 eV, respectively. Note that these four bonding blocks calculated in the acetonitrile case have their equivalent in the 3-butenenitrile case. Therefore, we attribute the observed *N<sub>a</sub>*, *N<sub>b</sub>*, and *N<sub>c</sub>* XPS lines of 3-butenenitrile (Figure 2) to Si-N=C-Si, CDB, and datively bonded C≡N moieties. The corresponding NEXAFS transitions, calculated in the acetonitrile case, have energies close to the ones measured experimentally in the 3-butenenitrile case (see Table 1), which ensures the self-consistency of our attributions. In our assignment procedure (see Table 1 and Figures 2 and 3), the relationship between NEXAFS and XPS is expressed by the common subscripts a, b/b', and c.

Thus, the NEXAFS  $\pi_a^*$  transition (397.4 eV) (corresponding to the XPS *N<sub>a</sub>* line at 397.8 eV) is assigned to a Si-C≡N-Si unit. For such a bonding, the C≡N  $\pi$ -bond is contained in the surface plane, and indeed, the NEXAFS  $\pi_a^*$  transition is polarized in the (001) plane. Acetonitrile (CH<sub>3</sub>-C≡N) also binds to silicon by forming such units, and an intense, (001) polarized,  $\pi^*$  transition is observed at 397.7 eV.<sup>4,17</sup>

The NEXAFS transitions to the two orthogonal  $\pi_b^*$  (398.6 eV) and  $\pi_b'^*$  (~402 eV) orbitals originate from a common core level, the XPS *N<sub>b</sub>* line at 398.8 eV. They have their exact counterpart (at 398.8 and ~402 eV) when the silicon surface is covered by 2-propenenitrile.<sup>4,6</sup> Therefore, for what concerns the presence of CDB products resulting from the adsorption of 3-butenenitrile and 2-propenenitrile on Si(001), IR<sup>5</sup> and NEXAFS spectroscopy are in complete agreement. Because  $\pi_b^*$

(respectively  $\pi_b'^*$ ) transition is polarized in the (001) plane (respectively along [001]), the CDB adduct lies flat on the surface.

The observation of a CDB adduct is unexpected, because 3-butenenitrile is not conjugated. Although not detected by NEXAFS in the multilayer film, the presence of a small concentration of 2-butenenitrile in the gas cannot be entirely excluded. If isomerization in the gas line were the only reaction path, the sticking coefficient of 2-butenenitrile on Si(001) should be several orders of magnitude greater than that of 3-butenenitrile, to account for the proportion of CDB species found on the surface (see Figure 3). This assumption on the sticking probability of 2-butenenitrile does not seem to be reasonable, as the sticking coefficient of 3-butenenitrile is estimated to be in the 0.3–0.6 range.<sup>18</sup> Note that the conjugated molecule 2-propenenitrile (Figure 1b) has also a sticking coefficient close to 1, judging from the kinetic data of ref 18. Consequently, reaction paths involving the silicon surface must be envisioned to account for the presence of the CDB species.

The attribution of the  $\pi_c^*$  transition (Figure 3) observed at 399.6 eV to a datively bonded cyano relies both on calculated NEXAFS transitions and IPs. Indeed, the pendent cyano and the datively bonded cyano have the same CN triple bond character and their calculated NEXAFS transition energies are very close. A distinction can only be made via a comparison of their calculated IPs. Indeed, the calculation shows that the donation of the nitrogen lone pair (the nitrogen becomes “more positive” with respect to that of the free cyano) induces a strong chemical shift to higher IP, about 1 eV, with respect to that of free cyano. Regarding the possibility that the nitrogen end is bonded to silicon, any calculated geometry must account for the weak X-ray absorption dichroism of peak  $\pi_c^*$  (see section III.D).

**B. Real-Time Resonant N KVV Auger Yield Measurements.** We have made the intriguing observation that a saturated surface is prone to evolve chemically during exposure to the 3-butenenitrile gas: NEXAFS spectra exhibit clear variations in the relative  $\pi^*$  level distribution depending on the overall exposure time. An illustrative case is reported in Figure 4. The beam-light incidence angle,  $\theta$ , is the magic angle (54.7°), chosen in order to make the measured intensity independent of the molecular orientation. Exposures have been made at constant pressure (10<sup>−8</sup> mbar): curve 4a is measured at a base pressure of 10<sup>−10</sup> mbar, following an exposure of 1080 s; curve 4b is measured after an extra exposure of 8000 s (total exposure time of 9080 s). Such exposures largely exceed surface saturation (see below), but it appears clearly that the  $\pi_a^*$  line (Si-C≡N-Si) decreases—respectively the  $\pi_b^*$  line (datively bonded C≡N) increases—with increasing exposure time to the gas.

Aware of such a surface evolution, we have carried out *real-time* N KVV Auger yield measurements in the presence of the

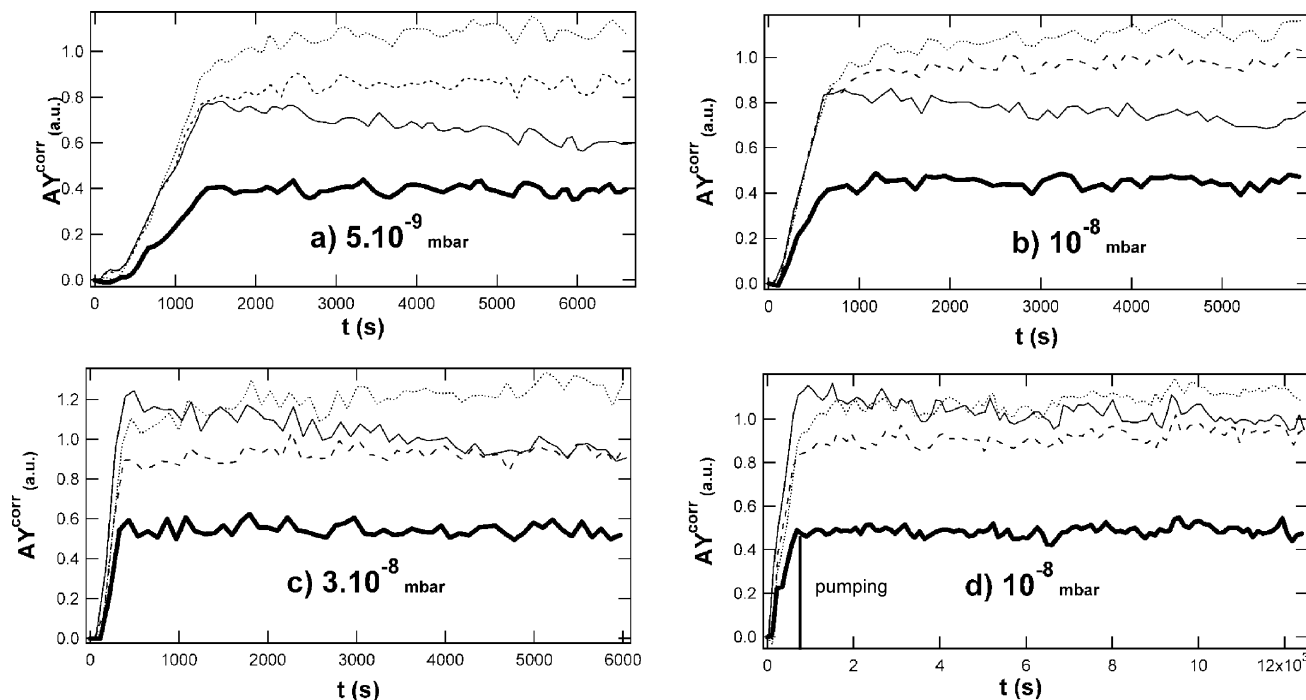


**Figure 5.** Resonant N KVV Auger kinetics. Four resonant structures are followed: continuum (bold continuous), Si—C=N—Si (continuous), CDB adduct (dashes), and datively bonded C≡N (dots).

**TABLE 2: Nitrogen Initial Uptake Rate,  $\dot{\Theta}_N^{\text{init}}$ , Saturation Time,  $\tau_{\text{sat}}$ , and Inverse Characteristic Time of the  $a \rightarrow c$  Transformation for  $t \geq \tau_{\text{sat}}$  ( $K_{a \rightarrow c}$ ) (These Values Are Extracted from the Real-Time AY Curves of Figure 7)**

curve	a	b	c	d
dose (mbar $\times$ s)	$5 \times 10^{-9} \times 6000$	$10^{-8} \times 6000$	$3 \times 10^{-8} \times 6000$	$10^{-8} \times 960 + \text{residual} \times 9000$
$\dot{\Theta}_N^{\text{init}}$ ( $\text{s}^{-1}$ )	$3.9 \times 10^{-4}$	$7.8 \times 10^{-4}$	$25.3 \times 10^{-4}$	$7.910^{-4}$
$\tau_{\text{sat}}$ (s)	1400	720	330	690
$K_{a \rightarrow c}$ ( $\text{s}^{-1}$ )	$5.2 \times 10^{-5}$	$3.2 \times 10^{-5}$	$4.7 \times 10^{-5}$	$9 \times 10^{-6}$
$K_{a \rightarrow c}^{-1}$ (h)	5.3	8.6	5.9	30.4

gas (the beamlight incidence was the “magic angle”). In Figure 5, we report, as a function of time,  $t$ , the corrected Auger yield intensities (see section II.A)  $AY_a^{\text{corr}}$ ,  $AY_b^{\text{corr}}$ ,  $AY_c^{\text{corr}}$ , and  $AY_{\text{cont}}^{\text{corr}}$  that are measured, respectively, at the energies of the  $\pi_a^*$  transition (Si—C=N—Si bonding),  $\pi_b^*$  transition (N=C=C),  $\pi_c^*$  (datively bonded C≡N), and at  $h\nu = 415$  eV (transition to the continuum). Note that  $AY_{\text{cont}}^{\text{corr}}$  (measured at  $h\nu = 415$  eV) is proportional to the amount of deposited N atoms on the surface.

Different kinds of experiments have been carried out:

- Exposures to the gas for 6000 s, under pressures of  $5 \times 10^{-9}$  (curve 5a),  $10^{-8}$  (curve 5b), and  $3 \times 10^{-8}$  mbar (curve 5c).
- Exposure for 1080 s under  $10^{-8}$  mbar, interrupted to record the NEXAFS spectrum (a) of Figure 4, followed by subsequent exposure of 8000 s, after which the NEXAFS spectrum (b) of Figure 4 was recorded.
- Exposure for 960 s under  $10^{-8}$  mbar, followed by pumping down to the base pressure ( $10^{-10}$  mbar) and NEXAFS monitoring for 9000 s, to examine the evolution of the 3-butenitrile covered surface in the residual vacuum (curve 5d).

Let us first focus on  $AY_{\text{cont}}^{\text{corr}}$ , which is proportional to the total N uptake. Examination of curves 5a–d shows that, for a given pressure, the total N uptake has a nearly constant rate until saturation is reached. This non-Langmuirian behavior suggests the presence of a molecular precursor on the surface.<sup>19</sup> We can define the normalized nitrogen uptake,  $\Theta_N$ , as the ratio  $AY_{\text{cont}}^{\text{corr}}(t)/(\max(AY_{\text{cont}}^{\text{corr}}))$  ( $\Theta_N$  is its time derivative). Let us define  $\tau_{\text{sat}}$ , the time at which saturation occurs, that is,  $\dot{\Theta}_N$  becomes zero. For the various pressures,  $\Theta_N$ ,  $\dot{\Theta}_N^{\text{init}}$  (the initial rate), and  $\tau_{\text{sat}}$  are collected in Table 2. The mechanistic interpre-

tation is given in Figure 6 (steps 1 and 2). One can notice that  $\dot{\Theta}_N^{\text{init}}$  increases linearly with the gas pressure in accord with the precursor model.<sup>19</sup>

Let us now examine the temporal behavior of  $AY_a^{\text{corr}}$ ,  $AY_b^{\text{corr}}$ , and  $AY_c^{\text{corr}}$  in curves 5a–c, corresponding to continuous exposures to the gas. For times  $t \leq \tau_{\text{sat}}$ , the corrected Auger yields of all three species increase linearly with time. This means that the molecular precursor is involved in three parallel reactions, with reaction constants of the same order of magnitude.

However, for times  $t \geq \tau_{\text{sat}}$ , while  $AY_b^{\text{corr}}$  (N=C=C) remains nearly constant, in contrast,  $AY_a^{\text{corr}}$  (Si—C=N—Si) decreases and  $AY_c^{\text{corr}}$  (C≡N) increases. This  $a \rightarrow c$  transformation occurs without any change in the nitrogen density on the surface.  $AY_{\text{cont}}^{\text{corr}}(t)$  is constant for  $t \geq \tau_{\text{sat}}$  ( $\Theta_N = 1$ ), this means that there is no measurable desorption/absorption. The NEXAFS spectra collected in Figure 4 give a confirmation of the trends observed with AY kinetics. The Si—C=N—Si species is converted into a C≡N unit. For  $t \geq \tau_{\text{sat}}$ ,  $AY_a^{\text{corr}}$  can be fitted by an exponentially decreasing law.

$$AY_a^{\text{corr}}(t) = AY_a^{\text{corr}}(\tau_{\text{sat}}) \exp(-K_{a \rightarrow c}(t - \tau_{\text{sat}})) \quad (1)$$

The  $K_{a \rightarrow c}$  values are reported in Table 2. Contrary to  $\dot{\Theta}_N^{\text{init}}$  which increases with pressure,  $K_{a \rightarrow c}$  is nearly constant (with respect to the measurement precision) in the studied pressure range and equal to  $(4 \pm 1) \times 10^{-5} \text{ s}^{-1}$ . Therefore, the characteristic transformation time of the Si—C=N—Si unit in the presence of the gas,  $K_{a \rightarrow c}^{-1}$ , is  $\sim 7$  h. On the other hand,

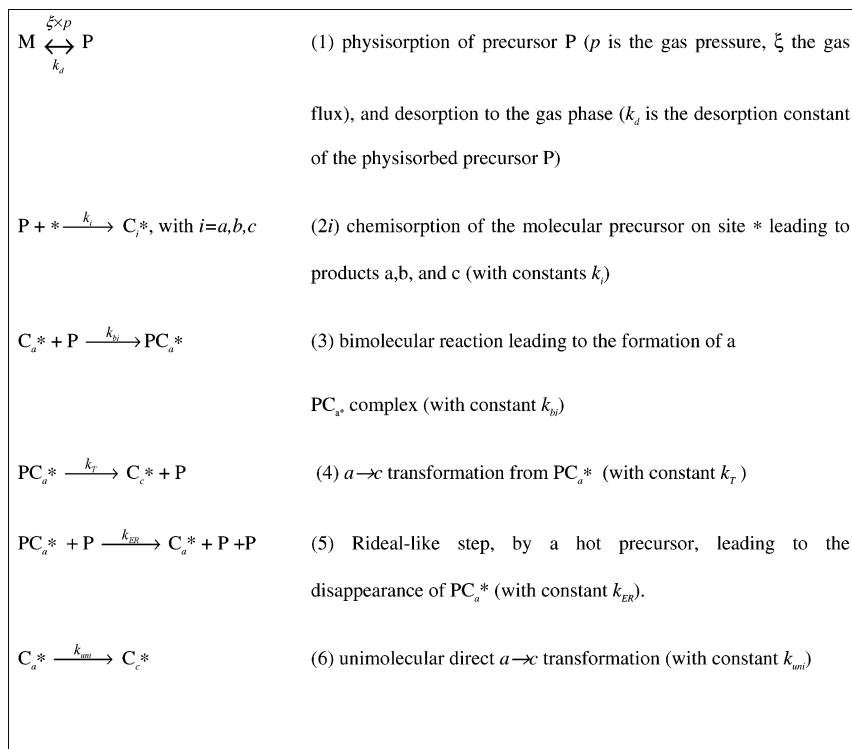


**Figure 6.** Reaction mechanisms of 3-butenitrile on silicon (001). M, P, and  $*$  designate a molecule in the gas phase, a physisorbed molecular precursor, and a chemisorption site, respectively. Steps 1 and 2 lead to the chemisorption of the three products detected by XPS/NEXAFS. Steps 3–5 describe the  $a \rightarrow b$  transformation which occurs on time scales much larger than  $\tau_{sat}$ . Steps 3 and 4 are necessary to explain why the  $a \rightarrow c$  transformation is accelerated by the exposure to the gas. An Eley–Rideal-like step (step 5) is also included in order to interpret why the measured  $K_{a \rightarrow c}$  constant does not depend on pressure in the  $5 \times 10^{-9}$  to  $3 \times 10^{-8}$  mbar range. Step 6 is unimolecular and may be effective in the residual vacuum ( $10^{-10}$  mbar).

curve 5d shows that the conversion of the Si–C=N–Si unit is strongly slowed when 3-butenitrile is repumped. In the residual vacuum,  $K_{a \rightarrow c}$  decreases to  $9 \times 10^{-6}$  s; that is, the characteristic time,  $K_{a \rightarrow c}^{-1}$ , is about 30 h. We have also checked by introducing a pressure of  $10^{-6}$  mbar of oxygen for 6000 s that the  $a \rightarrow c$  transformation is not accelerated by surface oxidation.

Therefore, we can conclude that the conversion of Si–C=N–Si (the  $C_a^*$  species of Figure 6) is catalyzed by 3-butenitrile molecules coming from the gas phase. The interaction of a physisorbed molecule (P) with  $C_a^*$  to form the complex  $PC_a^*$  can be envisaged (step 3 of Figure 6), with a subsequent transformation of  $C_a^*$  into  $C_c^*$  (step 4). With these assumptions, for  $t \geq \tau_{sat}$ , the reaction rate is

$$\frac{d}{dt}[C_a^*] = -k_{bi}[P][C_a^*] \quad (2)$$

where  $[P]$  is the surface concentration of physisorbed (precursor) molecules.

Then,  $K_{a \rightarrow c}$  can be written as

$$K_{a \rightarrow c} = k_{bi}[P] \quad (3)$$

Assuming for P a coverage much below saturation (a reasonable guess in the present range of pressures), then  $[P]$  is proportional to  $p$ , the pressure of 3-butenitrile. Consequently,  $K_{a \rightarrow c}$  should also be proportional to pressure, which is not observed in the  $5 \times 10^{-9}$  to  $3 \times 10^{-8}$  mbar pressure range.

The model needs some refinement to take this observation into account. One could consider an Eley–Rideal-like mechanism, by which the labile  $PC_a^*$  complex is destroyed by shocks with hot physisorbed molecules (Figure 6, step 5). Using the quasi-steady-state assumption, the  $PC_a^*$  concentration,  $[PC_a^*]$ ,

becomes equal to

$$[PC_a^*] = \frac{k_{bi}[P][C_a^*]}{k_T + k_{ER}[P]} \quad (4)$$

With the  $a \rightarrow c$  transformation rate satisfying the relation

$$\frac{d}{dt}[C_a^*] = -\frac{d}{dt}[C_c^*] = -k_T[PC_a^*] \quad (5)$$

the  $K_{a \rightarrow c}$  constant is equal to

$$K_{a \rightarrow c} = \frac{k_T k_{bi}[P]}{k_T + k_{ER}[P]} \quad (6)$$

In such a model,  $K_{a \rightarrow c}$  becomes nearly independent of pressure,  $p$ , when  $k_T \ll k_{ER}[P]$  and

$$K_{a \rightarrow c} = \frac{k_T k_{bi}}{k_{ER}} \quad (7)$$

This could explain the *pseudounimolecular* transformation rate in the  $5 \times 10^{-9}$  to  $3 \times 10^{-8}$  pressure range. On the other hand, when  $k_T \gg k_{ER}[P]$  (i.e., at a very low 3-butenitrile pressure,  $p$ ),  $K_{a \rightarrow c} \rightarrow k_{bi}[P]$ , similar to eq 3. The very slow transformation observed in a vacuum could be due to a very low partial pressure of the gas (below  $10^{-10}$  mbar), but a spontaneous unimolecular reaction (step 6 of Figure 6) cannot be excluded.

**C. STM Measurements.** The adsorption structure of 3-butenitrile on Si(001)- $2 \times 1$  was examined by STM. Exposures were all performed at room temperature. First, we present surface images obtained keeping the sample at 80 K,



## C. STM measurements.

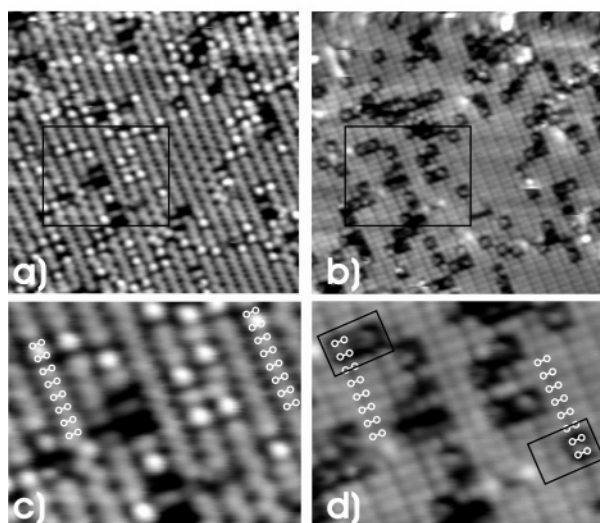


**Figure 7.** STM images of a Si(100)- $2 \times 1$  surface exposed to 3-butenitrile at room temperature (dose =  $5 \times 10^{-9}$  mbar  $\times$  10 s). The images are acquired keeping the substrate at 80 K: (a)  $V_b = -1.7$  V (filled-state image); (b)  $V_b = +1.7$  V (empty-state image). The tip current is 1 nA in both cases.

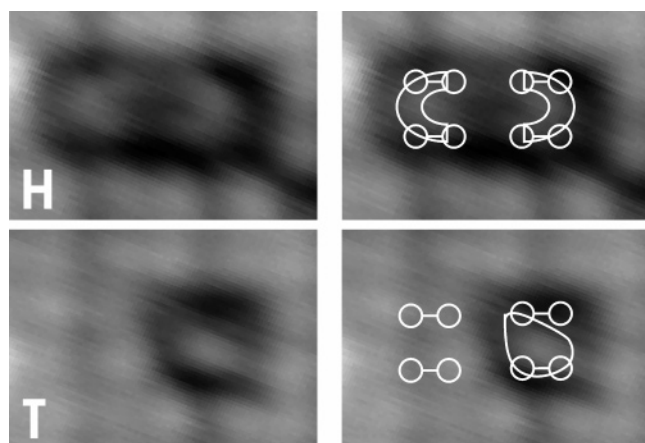


**Figure 8.** Zoomed areas (zones delimited by dark rectangles in Figure 8b), showing the occurrence of two adducts: (upper two panels) the “horseshoe”; (lower two panels) the “triangle”.

for which the spatial resolution was found to be better than that at 300 K. Figures 7 and 8 show images of a Si surface covered with a small amount of molecules (the exposure was  $5 \times 10^{-9}$  mbar  $\times$  10 s). Figure 7a is the filled-state image, acquired at a sample bias voltage,  $V_b$ , of  $-1.7$  V, while Figure 7b is the unoccupied-state image, in the same surface region, acquired at  $+1.7$  V. Parts c and d of Figure 7 are respectively zoomed areas of parts a and b of Figure 7. A scaled drawing depicting the silicon dimers (the white dumbbells) is superimposed onto the images. The dimer row center appears as a line protrusion in Figure 7c but as a line depression in Figure 7d. Static buckling is well observed in the filled-state image (the measurement is made below the dynamic-to-static buckling transition temperature 120 K<sup>21</sup>). However, in the unoccupied-state image, buckling is not imaged at  $V_b = +1.7$  V: instead, a symmetric double-lobed structure is seen very clearly. In fact, in unoccupied-state images, buckling appears when  $V_b$  is decreased to  $+0.9$  V, but at the expense of image resolution (not shown).

In the filled-state image (Figure 7c), molecules appear as white disk-shaped protrusions. The molecular imprint is nested in sites comprising two adjacent dimers in the same row. In

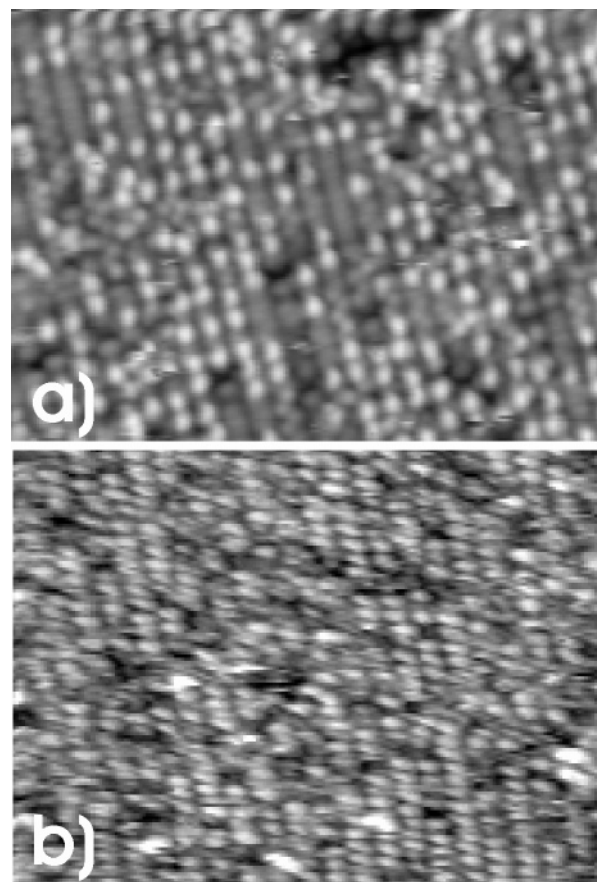


**Figure 9.** STM filled-state images of a Si(100)- $2 \times 1$  surface exposed to 3-butenitrile at room temperature. The doses are (a) 30 s under  $10^{-8}$  mbar and (b) 120 s at  $10^{-8}$  mbar. The images are acquired at 300 K for (a)  $I = 1$  nA and  $V_b = -3$  V and for (b)  $I = 0.3$  nA and  $V_b = -2$  V. The molecular imprint is still located within two adjacent dimers in the same row. Two adsorption sites can be contiguous.

filled-state images of the adsorbed molecules, neither can atom-size details be seen nor is there any hint for the occurrence of different reaction products.

On the other hand, atom-size resolution is enhanced in the unoccupied-state images (Figures 7d and 8). Molecular imprints are obtained with finer details, inserted within square depression, the latter being a strong indication that the two silicon dimers are reacted. Horseshoe-shaped imprints are clearly seen (a zoomed area is given in Figure 8a). Other molecular imprints (of triangular shape) can also be observed (Figure 8b).

We have also obtained images (filled-state images, the surface is imaged at room temperature) for coverages close to saturation: Figure 9a, half a monolayer; Figure 9b, close to saturation (the dose and scanning parameters are given in the caption). The molecular imprints in Figure 9a are still located within two adjacent dimers in the same row. Two (double-dimer) adsorption sites can be contiguous. It happens also that silicon dimers remain unreacted because they are placed between two double-dimer sites: apparently, adsorption on these dimers via only one anchoring unit (cyano or vinyl) cannot occur because of steric repulsion (only about 2% of the imprints, not centered above a double-dimer, could be other anchoring modes or impurities). In Figure 9b, the lack of resolution does not enable us to see if the remaining dimers are occupied by molecules with different adsorption modes, but the majority of the molecules seems to be adsorbed on double-dimer sites.

**D. Modeling the Adsorption Geometries.** The fact that the molecular adducts are exclusively inserted in surface sites

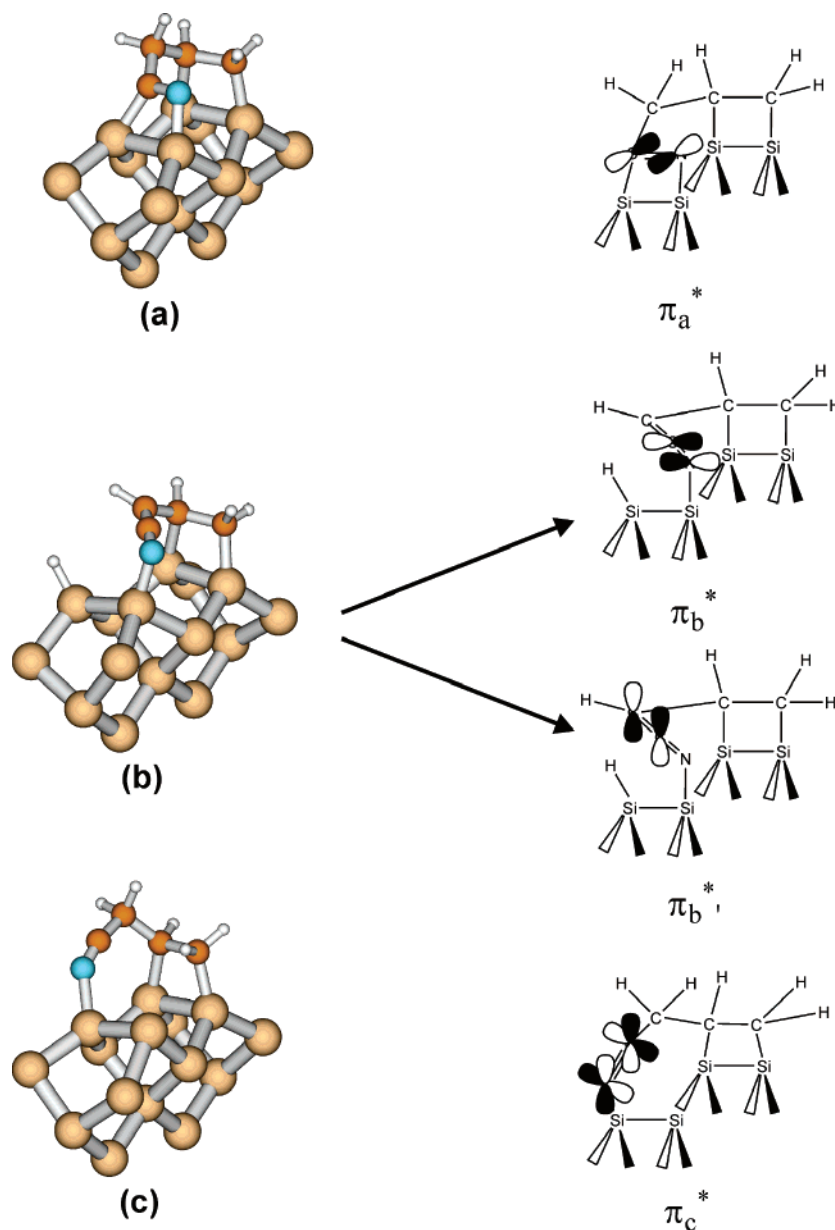


**Figure 10.** Calculated adsorption geometries<sup>23</sup> and scheme of the expected unoccupied orbitals of  $\pi$  symmetry: (a) In the double-cycloaddition geometry, the  $\pi_a^*$  orbital is parallel to the surface plane. (b) The CDB adduct plus silicon monohydride: the two mutually orthogonal transitions  $\pi_b^*$  and  $\pi_b'^*$  are formed. (c) The datively bonded  $\text{C}\equiv\text{N}$  leads to a triple bond  $\pi_c^*$ , whose axis makes an angle of  $55.6^\circ$  with respect to the normal to the surface, which explains the nondichroic behavior of the NEXAFS spectrum for this transition. Note that the H termination of the  $\text{Si}_{15}\text{H}_{16}$  cluster is omitted for clarity.

comprising two adjacent dimers in the same row is the main information provided by STM. This limits considerably the number of adsorption modes that can be envisaged. First, we can exclude one-dimer geometries, that is, adsorption via only one anchoring unit (cyano or vinyl), as well as CDB adducts “cycloadded” over one dimer after 3-butenitrile to 2-butenitrile isomerization as proposed by Mui et al. (ref 10). Second, STM images do not show the formation of reaction products spanning the trench between two dimer rows (the minimum distance between two silicon dangling bonds is  $\sim 5.5$  Å; see Figure 1a). This kind of site would allow the formation of CDB adducts. Indeed, in a STM study of 2-propenenitrile adsorption at low coverage we have recently carried out, we only observe a “cross-trench” bridging mode.<sup>6</sup> Given the similarity between 2-propenenitrile and 2-butenitrile (Figure 1b), these observations do not favor an isomerization of 3-butenitrile to 2-butenitrile before the formation of the molecular adduct.

As suggested by the STM images, one can first consider an adduct consisting of a molecule whose both anchoring (cyano and vinyl) units have reacted with two adjacent dimers in the same row. This is fully consistent with NEXAFS data that point to the formation of a  $\text{Si}-\text{C}\equiv\text{N}-\text{Si}$  unit having its  $\pi_a^*$  system contained in the surface plane (Figure 3) and with IR data<sup>5</sup> that show also that the vinyl moiety has reacted with silicon.<sup>22</sup> We propose that such a “double-cycloaddition” product (the calculated optimized geometry on a  $\text{Si}_{15}\text{H}_{16}$  cluster<sup>23</sup> is given in Figure 10a) corresponds to the “horseshoe” molecular imprint of Figure 8. For 3-butenitrile, no reaction path calculations are available, involving the di- $\sigma$  anchoring of both vinyl and cyano groups on the  $\text{Si}(001)-2 \times 1$  surface. It should be interesting to examine if their grafting occurs sequentially or in a concerted manner.<sup>24</sup>

The second adduct, the CDB, detected both by NEXAFS and IR spectroscopy, should also form on a double-dimer site. We



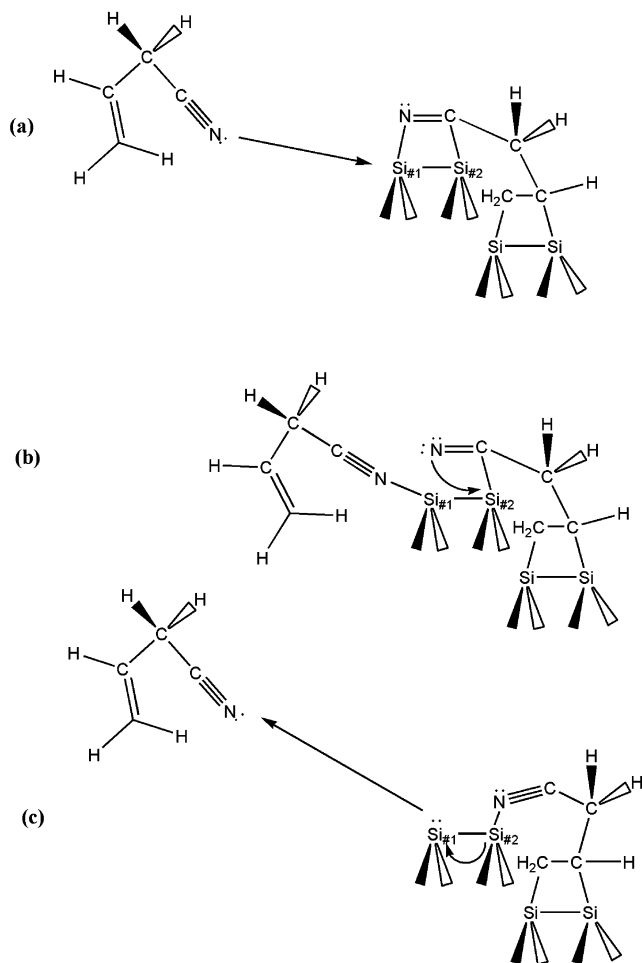


**Figure 11.** (a) Nucleophilic attack on Si<sub>#1</sub> (assumed to be electron deficient due to transfer to the CN moiety) by an extra physisorbed molecule. (b) Complex formation. (c) The cyano moiety of the chemisorbed adduct makes a dative bond with Si<sub>#2</sub> via donation of its nitrogen lone pair. Consequently, an electron pair is transferred to Si<sub>#1</sub>, inducing the departure of the extra 3-butenitrile molecule.

propose the following geometry: one silicon dimer still bonds to the vinyl; however, in contrast to the preceding geometry, one silicon atom of the adjacent dimer bonds to the nitrogen and the second one scavenges an  $\alpha$ H to form Si-H. A CDB unit results. The Si-H stretching wavenumber is in the range 2066 cm<sup>-1</sup> (ref 25) to 2090 cm<sup>-1</sup> (ref 26). In the IR spectrum of chemisorbed 3-butenitrile reported by Schwartz and Harmers,<sup>5</sup> vibrational intensity is seen at  $\sim$ 2070 cm<sup>-1</sup> as a shoulder of the CDB characteristic peak at 1982 cm<sup>-1</sup>. A peaked Si-H line may not be observed in the latter case, due to the lower proportion of CDB on the surface in their experiment (about 17% of the chemisorbed species, instead of about 40% in the present study). We give in Figure 10b the optimized geometry of a CDB embedded in the two-dimer site. The molecule lies flat on the surface, which is consistent with the NEXAFS data ( $\pi_b^*$  polarized in the surface plane,  $\pi_b^*$  orthogonal to the surface plane). Due to the fact that the N=C=C axis is roughly along the diagonal of the double-dimer site, a confrontation with the STM empty-state images suggests that it could be a candidate for the triangle-shaped molecular imprint of Figure 8.

The third adspecies detected by NEXAFS/XPS is a cyano moiety datively bonded to silicon. We propose a model in which the vinyl group is cycloadditioned onto a silicon dimer, while the cyano group donates its lone pair to a silicon dangling bond of

the neighboring dimer in the same row (Figure 10c). After geometry optimization, the calculated angle between the C≡N and the normal to the surface is 55.6°. Such a value, close to the magic angle (54.7°), accounts for the nondichroic behavior of the  $\pi_c^*$  NEXAFS line (Figure 3). Such an adsorption geometry could also compete for the attribution of the triangle-shaped molecular imprint of Figure 8.

From a mechanistic viewpoint, the key surface reaction site is the double-dimer site. Here, we expect a competition between nondissociative adsorption on one hand (the cyano-vinyl cycloaddition geometry and vinyl-cycloaddition geometry plus a datively bonded CN) and dissociative adsorption on the other hand (via  $\alpha$ H transfer to a silicon, leading to the formation of CDB + Si-H adducts). XPS shows that these products are found in comparable proportions at 300 K.

NEXAFS shows (Figures 4 and 5) that the double-cycloaddition product of Figure 10a is unstable when exposed to a continuous flux of 3-butenitrile: then, the Si-C=N-Si bond is transformed into a CN triple bond. In section III.B, we have considered the role of molecules physisorbed on the surface, making a complex with the cyano-vinyl anchored adduct. We attempt in Figure 11 to give an explanation for the observed transformation. We propose that there is enough room in the trench between dimer rows to enable a physisorbed molecule to direct its nitrogen lone pair toward a positively charged silicon (Si<sub>#1</sub>) of a Si-C=N-Si unit (Figure 11a). As a matter of fact, the low binding energy of N 1s pertaining to such a block is suggestive of a sizable electron transfer from silicon. Then, a complex (Figure 11b), whose presence is suggested by the kinetic data (section III.B), forms. The dative bond formed by the cyano group of the chemisorbed adduct on Si<sub>#2</sub> induces an electron transfer to Si<sub>#1</sub>, so that the extra molecule is repelled from the site (Figure 11c).

#### IV. Conclusion

Using NEXAFS, XPS, and STM techniques in combination, we have studied the surface reactions of 3-butenitrile on Si-(001)-2  $\times$  1 at room temperature. N 1s NEXAFS and XPS spectra of the molecules chemisorbed at 300 K point to the occurrence of three different bonding geometries on the surface characterized, respectively, by a reacted cyano (Si-C=N-Si), a C≡N unit datively bonded to silicon, and, in accord with ref 5, a CDB (C=C=N) unit. We have checked that the CDB formation is not due to an experimental artifact (isomerization in the gas line before adsorption on the surface) by measuring the NEXAFS N 1s spectrum of a condensed multilayer. STM images point to multiple bonding geometries. In all cases, an adsorption site is constituted by two adjacent dimers in the same row. This points to a remaining cis conformation of the molecule on the silicon surface. The good atomic resolution obtained at positive biases (unoccupied states) and low measurement temperature enables the observation of horseshoe-shaped molecular imprints, that we attribute to the reaction of both anchoring units (vinyl and cyano) to two adjacent silicon dimers. The models we propose for the other adsorption modes detected by our spectroscopic techniques (they may correspond to the triangle-shaped molecular imprints of the STM images) also involve two adjacent dimers in the same row as the surface adsorption site. For the CDB adduct, we propose that the adduct is still nested in a double-dimer site. At variance with previous models<sup>5</sup> and calculations,<sup>10</sup> we assume that one  $\alpha$ H is transferred to a silicon dangling bond and not to a  $\gamma$ C carbon to form a 2-butenitrile intermediate.

Real-time NEXAFS shows that the Si-C=N-Si unit is prone to transformation into a C≡N unit in the presence of 3-butenitrile.

itrile gas, we discuss the role of the physisorbed molecule in this catalytic reaction.

**Acknowledgment.** The authors wish to thank Professor Robert A. Bartynski for reading this manuscript.

## References and Notes

- (1) Bent, S. F. *Surf. Sci.* **2002**, *500*, 879.
- (2) Bent, S. F. *J. Phys. Chem. B* **2002**, *106*, 2830.
- (3) Filler, M. A.; Bent, S. F. *Prog. Surf. Sci.* **2003**, *73*, 1.
- (4) Bournel, F.; Gallet, J.-J.; Kubsky, S.; Dufour, G.; Rochet, F.; Simeoni, M.; Sirotti, F. *Surf. Sci.* **2002**, *513*, 37.
- (5) Schwartz, M. P.; Hamers, R. J. *Surf. Sci.* **2002**, *515*, 75.
- (6) Rangan, S.; Kubsky, S.; Gallet, J.-J.; Bournel, F.; Le Guen, K.; Dufour, G.; Rochet, F.; Funke, R.; Knepe, M.; Piaszenski, G.; Köhler, U.; Sirotti, F. *Phys. Rev. B* **2005**, *71*, 125320.
- (7) Schei, S. H. *J. Mol. Struct.* **1983**, *98*, 141.
- (8) A situation encountered for 1,4-pentadiene for which only one of the two vinyl groups reacts. See: Bournel, F.; Jolly, F.; Rochet, F.; Dufour, G.; Sirotti, F.; Torelli, P. *Phys. Rev. B* **2000**, *62*, 7645.
- (9) Filler, M. A.; Mui, C.; Musgrave, C. B.; Bent, S. F. *J. Am. Chem. Soc.* **2003**, *125*, 4928.
- (10) Mui, C.; Filler, M. A.; Bent, S. F.; Musgrave, C. B. *J. Phys. Chem. B* **2003**, *107*, 12256.
- (11) Donation of a pseudo- $\pi$  orbital on the  $\alpha$ C to the  $\pi^*$  orbital of the triple bond weakens the C–H bond.
- (12) Sirotti, F.; Polack, F.; Cantin, J.-L.; Sacchi, M.; Delaunay, R.; Meyer, M.; Liberati, M. *J. Synchrotron. Radiat.* **2000**, *7*, 5.
- (13) See: Stöhr, J. *NEXAFS Spectroscopy*, 2nd ed.; Springer: 1998; p 114.
- (14) The substrate symmetry must be greater than 3, which is the case for a  $2 \times 1/1 \times 2$  reconstructed surface. For further details, see: Stöhr, J. *NEXAFS Spectroscopy*, 2nd ed.; Springer: 1998; pp 284–285.
- (15) The C 1s XPS spectrum measured at  $h\nu = 330$  eV (not shown) can be fitted with two peaks at 284.8 eV (85% of the spectral weight) and at 286.5 eV (15% of the spectral weight). The broad main peak (1.4 eV fwhm) accounts for the two energetically close structures placed at 284.4 eV (0.86 eV fwhm and spectral weight of 31%) and 285.1 eV (0.95 eV fwhm and spectral weight of 64%) in ref 5. Note that in the present case the high binding peak has a larger spectral weight than the corresponding one placed at 286.8 eV (spectral weight of 5%) in ref 5. As for the N 1s spectrum, the spectral lines are peaked at nearly the same energy in both works and only the relative intensities differ, due to a different distribution of the products.
- (16) See: Stöhr, J. *NEXAFS Spectroscopy*, 2nd ed.; Springer: 1998; p 279.
- (17) Rangan, S.; Bournel, F.; Gallet, J.-J.; Kubsky, S.; Le Guen, K.; Dufour, G.; Rochet, F.; Sirotti, F.; Carniato, S.; Ilakovac, V. *Phys. Rev. B* **2005**, *71*, 165319.
- (18) The flux,  $F$ , of 3-butenenitrile impinging on the surface at 300 K is  $F = 1.94 \times 10^{20} \times p_{\text{nom}} \times G^{-1}$  molecules $\cdot\text{cm}^{-2}\cdot\text{s}^{-1}$ , where  $p_{\text{nom}}$  is the nominal pressure in millibars (calibrated for  $\text{N}_2$ ) and  $G$  is the ion gauge sensitivity factor. For propane and benzene,  $G$  is respectively equal to 4.2 and 5.8 (R. L. Summers, NASA Technical Note TN D-5285 National Aeronautics and Space Administration, Washington, DC, 1969). For 3-butenenitrile, the  $G$  factor cannot be found in the literature, but a value of  $\sim 5$  should be reasonable. At  $p_{\text{nom}} = 10^{-8}$  mbar, surface saturation occurs after an exposure of 720 s (the nitrogen adsorption rate is constant until saturation is reached); this corresponds to a dose of  $1.4 \times 10^{15} \times G^{-1}$  molecules $\cdot\text{cm}^{-2}$ , that is,  $\sim 2.8 \times 10^{14}$  molecules $\cdot\text{cm}^{-2}$ . The surface density of silicon dimers is  $3.4 \times 10^{14}$  atoms $\cdot\text{cm}^{-2}$ . Considering that the adsorption site of 3-butenenitrile comprises two silicon dimers (see section III.C), the sticking coefficient of 3-butenenitrile is  $\sim 0.6$  (if the adsorption rate of 2-butenenitrile is negligible). It would be  $\sim 0.3$  if the adsorption rate of 2-butenenitrile is assumed to be equal to that of 3-butenenitrile.
- (19) Chuan Kang, H.; Weinberg, W. H. *Surf. Sci.* **1993**, *299*, 755.
- (20) Ignoring the effect of steps 3–5 (see Figure 8), the time derivative of the surface concentration of the species  $C_i$  in the initial adsorption regime ( $t \leq \tau_{\text{sat}}$ ) is  $(d/dt)[C_i] \approx k_i \xi p / \sum_j k_j$ , for  $k_d \ll k_i$ . The time derivative of the total molecule concentration is  $(d/dt)\sum_i [C_i] \approx \xi p$ , and therefore,  $\Theta_{\text{N}}^{\text{init}}$  is proportional to  $p$ .
- (21) Wolkow, R. *Phys. Rev. Lett.* **1992**, *68*, 2636.
- (22) The grafting of the vinyl unit is similar to the bonding of ethylene on Si(001). In solid ethylene, an intense  $\pi_{\text{C}=\text{C}}^*$  C 1s NEXAFS peak is found at  $h\nu = 284.5$  eV. After adsorption on the surface, ethylene is rehybridized from  $\text{sp}^2$  to  $\text{sp}^3$ , and only a weak  $\sigma_{\text{C}-\text{Si}}^*$  transition is seen at 285.6 eV [Matsui, F.; Yeom, H. W.; Matsuda, I.; Ohta, T. *Phys. Rev. B* **2000**, *62*, 5036]. In the present case, we therefore expect transitions at 284.5 eV (respectively 285.6 eV) for the unreacted (respectively reacted) vinyl moiety. During the C 1s NEXAFS measurement, the absorption features expected around  $h\nu = 285$  eV were weak compared to the monochromator transmission “dip” at  $h\nu = 284.7$  eV (due to the presence of graphitic carbon on the optics), so that the normalization procedure (see section II.A) could not be carried out properly.
- (23) Electronic structure calculations are completed with the GAMESS software package (<http://www.msg.ameslab.gov/GAMESS/GAMESS.html>.) using the Becke3 Lee–Yang–Parr (B3LYP) three parameter DFT theory. Geometries of local minima on the potential energy surface were calculated with a SBKJ-C + 1d set for silicon, carbon, and nitrogen atoms and a 3-21-1p set for hydrogen. The Si(001)- $2 \times 1$  surface is modeled with a  $\text{Si}_{15}\text{H}_{16}$  cluster, corresponding to two adjacent dimers in the same row. The top two silicon atoms compose the surface dimer, while the remaining 13 Si atoms compose three subsurface layers which are hydrogen terminated to preserve the  $\text{sp}^3$  hybridization of the bulk diamond lattice. Geometrical constraints were applied to the five bottom atoms of the cluster to simulate a bulk environment.
- (24) The calculations of 2-propenenitrile reaction paths, using silicon clusters in Mui et al. (ref 10) and embedded clusters in Choi and Gordon (Choi, C. H.; Gordon, M. S. *J. Am. Chem. Soc.* **2002**, *124*, 6162), suggest that di- $\sigma$  cyano bonding is more favorable kinetically than di- $\sigma$  vinyl bonding.
- (25) Cao, X.; Hamers, R. J. *J. Vac. Sci. Technol., B* **2002**, *20*, 1614.
- (26) Chabal, Y. J.; Ragavachari, K. *Phys. Rev. Lett.* **1984**, *53*, 282.